

## Stability of biskyrmions in centrosymmetric magnetic films

Daniel Capic, Dmitry A. Garanin, and Eugene M. Chudnovsky

*Physics Department, Herbert H. Lehman College and Graduate School, The City University of New York,  
250 Bedford Park Boulevard West, Bronx, New York 10468-1589, USA*



(Received 21 January 2019; published 24 July 2019)

Motivated by the observation of biskyrmions in centrosymmetric magnetic films [X. Z. Yu *et al.*, *Nat. Commun.* **5**, 3198 (2014), W. Wang *et al.*, *Adv. Mater.* **28**, 6887 (2016)], we investigate analytically and numerically the stability of biskyrmions in films of finite thickness, taking into account the nearest-neighbor exchange interaction, perpendicular magnetic anisotropy (PMA), dipole-dipole interaction (DDI), and the discreteness of the atomic lattice. The biskyrmion is characterized by the topological charge  $Q = 2$ , the spatial scale  $\lambda$ , and another independent length  $d$  that can be interpreted as a separation of two  $Q = 1$  skyrmions inside a  $Q = 2$  topological defect in the background of uniform magnetization. We find that biskyrmions with  $d$  of order  $\lambda$  can be stabilized by the magnetic field within a certain range of the ratio of PMA to DDI in a film having a sufficient number of atomic layers  $N_z$ . The shape of biskyrmions has been obtained by the numerical minimization of the energy of interacting spins in a  $1000 \times 1000 \times N_z$  atomic lattice. It is close to the exact solution of the Belavin-Polyakov model when  $d$  is below the width of the ferromagnetic domain wall. We compute the magnetic moment of a biskyrmion and discuss ways of creating biskyrmions in experiment.

DOI: [10.1103/PhysRevB.100.014432](https://doi.org/10.1103/PhysRevB.100.014432)

### I. INTRODUCTION

Magnetic skyrmions in 2D films represent a very active field of research due to their potential for topologically protected data storage and information processing at the nanoscale [1–6]. Skyrmions were initially introduced in high-energy physics as nonlinear field models of elementary particles [7–9]. They entered condensed-matter physics after it was realized that Skyrme theory described topological defects in ferro- and antiferromagnetic films [10–12]. Similar topology leads to skyrmions in Bose-Einstein condensates [13], quantum Hall effect [14,15], anomalous Hall effect [16], and liquid crystals [17].

Skyrmions are characterized by the topological charge  $Q = \pm 1, \pm 2, \dots$ . In a 2D exchange model of a continuous spin field, the conservation of  $Q$  is provided by topology: Different  $Q$  arise from different homotopy classes of the mapping of the three-component fixed-length spin field onto the 2D plane. Similar topological properties are possessed by the magnetic bubbles that have been intensively studied in 1970s [18,19]. They were in effect cylindrical domains surrounded by domain walls of thickness  $\delta$  that is small compared to the radius of the domain  $R$ . In typical ferromagnets,  $\delta \sim 10\text{--}100$  nm, so the bubbles of the 1970s were at least of a micron size or greater. With the emergence of nanoscience- and nanoscale-measuring techniques, the experimentalists have been able to observe topological defects in 2D magnetic films of size smaller than  $\delta$ . This is when the field of “skyrmionics” took off in condensed-matter physics. Unlike the bubbles, nanoscale skyrmions are much closer to the topological defects described by the Skyrme model.

Research on magnetic skyrmions has focused on their stability, dynamics, and various symmetry properties. Perpendicular magnetic anisotropy (PMA), dipole-dipole interaction

(DDI), magnetic field, and confined geometry can stabilize significantly large magnetic bubbles [20–24]. For small skyrmions, violation of the scale invariance by the crystal lattice with a finite atomic spacing  $a$  leads to a stronger violation of the conservation of  $Q$ . In a pure exchange model, ferromagnetic skyrmions of size  $\lambda$  collapse [25] on a timescale proportional to  $(\lambda/a)^5$ . Their stability requires other than Heisenberg exchange coupling, strong random field, or random anisotropy, or, most commonly, a noncentrosymmetric system with large Dzyaloshinskii-Moriya interaction (DMI) [4,26–34].

To date, the presence of stable biskyrmions (see the computer-generated image in Fig. 1) has been independently reported at least in two centrosymmetric films of finite thickness: the  $\text{La}_{2-2x}\text{Sr}_{1+2x}\text{Mn}_2\text{O}_7$  manganite [35] and the  $(\text{Mn}_{1-x}\text{Ni}_x)_{65}\text{Ga}_{35}$  half Heusler alloy [36]. Given that stability of  $Q = 1$  skyrmions in films of large lateral dimensions normally require DMI, these findings are quite amazing and call for a theoretical analysis. Previously, we have shown [37] that clusters with  $Q > 1$  are naturally generated due to the presence of Bloch lines in domain walls when labyrinth domains are destroyed by the magnetic field in a centrosymmetric magnetic film of finite thickness. We also observed that  $Q = 2$  biskyrmions were generated by slow relaxation of the system at  $T = 0$  starting from the disordered spin state or, equivalently, by slow cooling to  $T = 0$  from high temperature. A more detailed numerical investigation of biskyrmions, including the current-induced dynamics, was performed in Ref. [38] within a 2D frustrated micromagnetic model. Biskyrmions arising from frustrated Heisenberg exchange have also been reported in studies of triangular spin lattices [31] and in Ginzburg-Landau theory of skyrmions [34]. Metastable biskyrmion configurations have been observed in Landau-Lifshitz dynamics of a frustrated bilayer

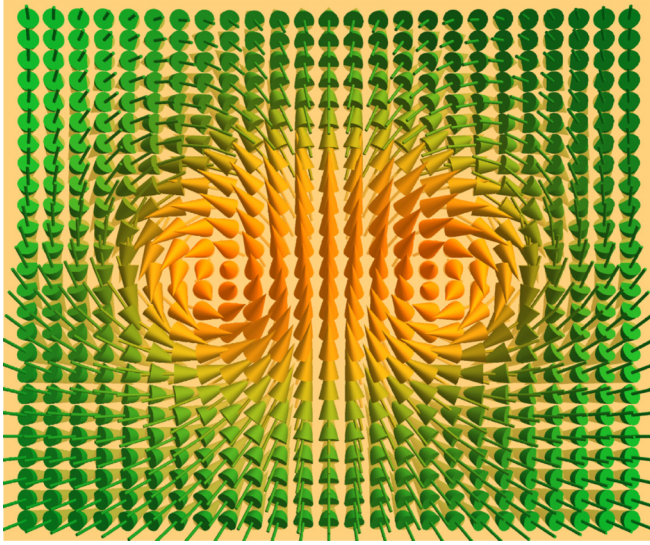


FIG. 1. Computer-generated spin field in a Bloch-type biskyrmion in a ferromagnetic film.

film [39]. However, the study of the separation of skyrmions in a biskyrmion, the shape of the biskyrmion, and its stability on the applied magnetic field, on the strength of the DDI, and on the film thickness in centrosymmetric systems has been absent so far. This, together with the above-mentioned experimental findings, provided motivation for our paper.

In the past, biskyrmions have been intensively studied in nuclear physics in a hope that they would provide a model of a deuteron [40,41]. The Belavin-Polyakov (BP) pure exchange model [10] in 2D contains an exact solution with  $Q = 2$  characterized by an arbitrary spatial dimension  $\lambda$ , and another arbitrary parameter  $d$  that can be visually interpreted as a separation of two  $Q = 1$  skyrmions in a  $Q = 2$  topological defect (see Fig. 1), although the nonlinearity of the model makes such interpretation meaningful only at a large separation. At  $d = 0$ , the defect possesses symmetry with respect to the rotation in the  $xy$  plane, which gets broken by any  $d \neq 0$ . We derive analytical formulas for the spin components and the magnetic moment of a BP biskyrmion for arbitrary  $\lambda$  and  $d$ .

In real systems, the magnetic biskyrmions are more complicated, as they are formed by a number of competing interactions. In this paper, we show that a biskyrmion spin configuration naturally arises from the energy minimization in a centrosymmetric film of finite thickness in a lattice model that contains nearest-neighbor exchange interaction, PMA, and DDI. In accordance with the experimental findings, we find that stable biskyrmions exist within a certain range of parameters in films of sufficient thickness.

One interesting observation that follows from our studies is that the DDI always favors a biskyrmion with a finite  $d$  over a  $Q = 2$  topological defect that does not split into  $Q = 1$  skyrmions. Another interesting observation is that, although biskyrmions are stabilized by interactions other than ferromagnetic exchange, sufficiently small biskyrmions are always close to the BP shape. On changing the parameters and the external magnetic field, one can change the shape of the  $Q = 2$  topological defect from a BP biskyrmion to a thin-wall biskyrmion bubble.

This paper is organized as follows. Analytical formulas for the spin components, the magnetic moment of a  $Q = 2$  skyrmion in a continuous spin-field BP exchange model, as well as the effect of the discreteness of the lattice are derived in Sec. II. Numerical results on biskyrmions in a lattice model of a centrosymmetric film of finite thickness with the nearest-neighbor exchange interaction, PMA, DDI, and the external magnetic field are presented in Sec. III. Our results and suggestions for experiments are discussed in Sec. IV.

## II. SKYRMIONS AND BISKYRMIONS IN THE 2D EXCHANGE MODEL

### A. Spin field in a Belavin-Polyakov (BP) biskyrmion

We begin with a 2D exchange model with the energy

$$E_{\text{ex}} = \frac{J}{2} \int dx dy (\nabla s_\alpha \cdot \nabla s_\alpha), \quad (1)$$

where summation over spin components  $\alpha = x, y, z$  is assumed. Here  $J$  is the exchange constant and  $\mathbf{s}$  is a three-component fixed-length spin field,  $\mathbf{s}^2 = 1$ . All spin-field configurations  $\mathbf{s}(x, y)$  are divided into homotopy classes characterized by the topological charge [10],

$$Q = \int \frac{dx dy}{4\pi} \mathbf{s} \cdot \frac{\partial \mathbf{s}}{\partial x} \times \frac{\partial \mathbf{s}}{\partial y}, \quad (2)$$

that takes quantized values  $Q = 0, \pm 1, \pm 2, \dots$ . The extremal spin-field configurations satisfy

$$\mathbf{s} \times \nabla^2 \mathbf{s} = 0. \quad (3)$$

Throughout this paper, we choose uniform magnetization,  $\mathbf{s} = (0, 0, -1)$ , in the negative  $z$  direction at infinity.

The absolute energy minimum inside each homotopy class is given by

$$E_{\text{ex}} = 4\pi J |Q|. \quad (4)$$

The corresponding solutions with  $Q > 0$  are called skyrmions, while solutions with  $Q < 0$  are called antiskyrmions. They have the simplest form [10,11] in terms of a complex variable  $\omega = \omega_1 + i\omega_2$  with

$$\omega_1 = \frac{2s_x}{1 + s_z}, \quad \omega_2 = \frac{2s_y}{1 + s_z}. \quad (5)$$

Equation (3) then reduces to  $\partial\omega/\partial x = \mp i\partial\omega/\partial y$  or, equivalently, to

$$\frac{\partial\omega_1}{\partial x} = \pm \frac{\partial\omega_2}{\partial y}, \quad \frac{\partial\omega_1}{\partial y} = \mp \frac{\partial\omega_2}{\partial x} \quad (6)$$

that corresponds to the Cauchy-Riemann conditions for the complex function  $\omega$ . They are satisfied by any analytical function  $\omega(z)$ , where  $z = x + iy$ .

The minimum-energy solutions for a skyrmion with  $Q = 1$  and an antiskyrmion with  $Q = -1$  are given by  $\omega = z/l$  and  $\omega = z^*/l$ , respectively, with  $z^*$  being the complex conjugate of  $z$ . The minimum-energy biskyrmion with  $Q = 2$  corresponds to

$$\omega(z) = e^{i\gamma} \frac{(z - d/2)(z + d/2)}{l^2} = e^{i\gamma} \frac{[z^2 - (d/2)^2]}{l^2}. \quad (7)$$

It is parametrized by the chirality angle  $\gamma$  and two lengths: the parameter  $l$  that roughly describes the size of the biskyrmion, and another parameter  $d$  that can be visually interpreted as the separation of two  $Q = 1$  skyrmions in a biskyrmion, see Fig. 1. Notice that the nonlinearity of Eq. (3) does not support this interpretation *per se*; rather, Eq. (7) suggests that a biskyrmion is a product of two  $Q = 1$  skyrmions.

In terms of  $\omega$  of Eqs. (5), the components of  $\mathbf{s}$  are given by

$$s_x = \frac{\text{Re}(\omega)}{1 + |\omega|^2/4}, \quad s_y = \frac{\text{Im}(\omega)}{1 + |\omega|^2/4}, \quad s_z = \frac{1 - |\omega|^2/4}{1 + |\omega|^2/4}. \quad (8)$$

These formulas allow one to obtain the spatial dependence of the components of the spin field in the BP biskyrmion:

$$s_x = \frac{2\lambda^2(x^2 - y^2 - d^2/4) \cos \gamma - 4\lambda^2 xy \sin \gamma}{\lambda^4 + (x^2 + y^2 - d^2/4)^2 + d^2 y^2}, \quad (9)$$

$$s_y = \frac{2\lambda^2(x^2 - y^2 - d^2/4) \sin \gamma + 4\lambda^2 xy \cos \gamma}{\lambda^4 + (x^2 + y^2 - d^2/4)^2 + d^2 y^2}, \quad (10)$$

$$s_z = \frac{\lambda^4 - (x^2 + y^2 - d^2/4)^2 - d^2 y^2}{\lambda^4 + (x^2 + y^2 - d^2/4)^2 + d^2 y^2}, \quad (11)$$

where we have replaced  $l$  with  $\lambda$ , satisfying  $\lambda^4 = 4l^4$  to have fewer numerical factors in the formulas.

Figure 1 provides visualization of the spin field given by the above equations with  $\gamma = \pi/2$  (Bloch-type biskyrmion). At the saddle point  $x = y = 0$ , one has

$$s_z = s_{z,\text{sad}} = \frac{\lambda^4 - (d/2)^4}{\lambda^4 + (d/2)^4}. \quad (12)$$

For  $d \gg \lambda$ , the BP biskyrmion becomes a superposition of two  $Q = 1$  BP skyrmions with the size  $\tilde{\lambda} = \lambda^2/d \ll \lambda$ .

For a biantiskyrmion, Eq. (7) with  $z \rightarrow z^*$  yields the expression similar to Eqs. (9)–(11) with the sign of the  $xy$  terms changed.

At  $d = 0$ , Eqs. (9)–(11) acquire a simple form in the polar coordinates,  $\mathbf{r} = (r, \phi)$ ,

$$\mathbf{s}(\mathbf{r}) = \left\{ \frac{2\lambda^2 r^2 \cos(\gamma \pm 2\phi)}{\lambda^4 + r^4}, \frac{2\lambda^2 r^2 \sin(\gamma \pm 2\phi)}{\lambda^4 + r^4}, \frac{\lambda^4 - r^4}{\lambda^4 + r^4} \right\}, \quad (13)$$

with a plus sign for the  $Q = 2$  skyrmion and a minus sign for the  $Q = -2$  antiskyrmion.

In a particular case of a compact single-centered  $|Q| = 2$  topological defect that does not split into  $Q = \pm 1$  skyrmions or antiskyrmions and is given by

$$\omega = e^{i\gamma} (z/l)^{|Q|}, \quad \omega = e^{i\gamma} (z^*/l)^{|Q|}, \quad (14)$$

respectively, one arrives at a more general expression that is valid for an arbitrary positive or negative integer  $Q$ :

$$\mathbf{s}(\mathbf{r}) = \left\{ \frac{2\lambda^{|Q|} r^{|Q|} \cos(\gamma + Q\phi)}{\lambda^{2|Q|} + r^{2|Q|}}, \frac{2\lambda^{|Q|} r^{|Q|} \sin(\gamma + Q\phi)}{\lambda^{2|Q|} + r^{2|Q|}}, \frac{\lambda^{2|Q|} - r^{2|Q|}}{\lambda^{2|Q|} + r^{2|Q|}} \right\}. \quad (15)$$

To determine the size  $\lambda$  of such a skyrmion from the numerically computed spin field, one can use the integrals that can

be obtained with the help of Eqs. (15):

$$I_1 = S_z = 2\pi \int r dr [s_z(r) + 1] = \frac{2\pi^2 \lambda^2}{|Q| \sin(\pi/|Q|)} \quad (16)$$

for  $|Q| \geq 2$  and

$$I_2 = 2\pi \int r dr [s_z(r) + 1]^2 = \frac{4\pi^2 \lambda^2 (|Q| - 1)}{Q^2 \sin(\pi/|Q|)}, \quad (17)$$

etc. Note that  $I_1$  is the total spin,  $S_z$ , of the topological defect (see below). If the values of  $\lambda_n$  obtained through different  $I_n$  are close to each other, the shape of the skyrmion is close to the BP shape. For  $Q = \pm 1$ , the first integral logarithmically diverges and one has to use  $I_n$  with higher powers of  $n$  to characterize the shape of the bubble (see, e.g., Eq. (8) of Ref. [42]).

The energy of any spin configuration can be computed with the help of Eq. (1) or by noticing its equivalent form

$$E = J \int dxdy \frac{|d\omega/dz|^2}{(1 + |\omega|^2/4)^2}. \quad (18)$$

Substitution of Eqs. (7) or (14) into Eq. (18) and integration with  $dxdy = r dr d\phi$  and  $z = x + iy = re^{i\phi}$  reproduces Eq. (4).

## B. Magnetic moment of the BP biskyrmion

The magnetic moment of the topological defect equals  $g\mu_B S_z$ , where  $g$  is the gyromagnetic factor,  $\mu_B$  is the Bohr magneton and  $S_z$  is the total spin of the defect defined as the difference between the spin of the 2D plane with and without the defect. For the boundary condition  $s_z = -1$  at infinity one has

$$S_z = \int \frac{dxdy}{a^2} (s_z + 1), \quad (19)$$

where  $a$  is the lattice constant and  $s_z$  is given by the last of Eqs. (8), which yields

$$s_z + 1 = \frac{2}{1 + |\omega|^2/4}. \quad (20)$$

For a biskyrmion given by Eq. (7) with  $l^2 = \lambda^2/2$ , switching to polar coordinates, one has

$$|\omega|^2/4 = u^2 - 2pu \cos(2\phi) + p^2, \quad u \equiv \frac{r^2}{\lambda^2}, \quad p \equiv \frac{d^2}{4\lambda^2} \quad (21)$$

Substituting this into Eqs. (20) and (19), one obtains

$$S_z = \left(\frac{\lambda}{a}\right)^2 f(p), \quad (22)$$

where

$$f(p) = \int_0^\infty \int_0^{2\pi} \frac{dud\phi}{u^2 - 2pu \cos(2\phi) + p^2 + 1}. \quad (23)$$

Integration over the angle yields

$$f(p) = 2\pi \int_0^\infty \frac{du}{[(u^2 - p^2 + 1)^2 + 4p^2]^{1/2}} \quad (24)$$

For an arbitrary  $p$ , this integral can be expressed via special functions in a rather cumbersome way that we do not provide

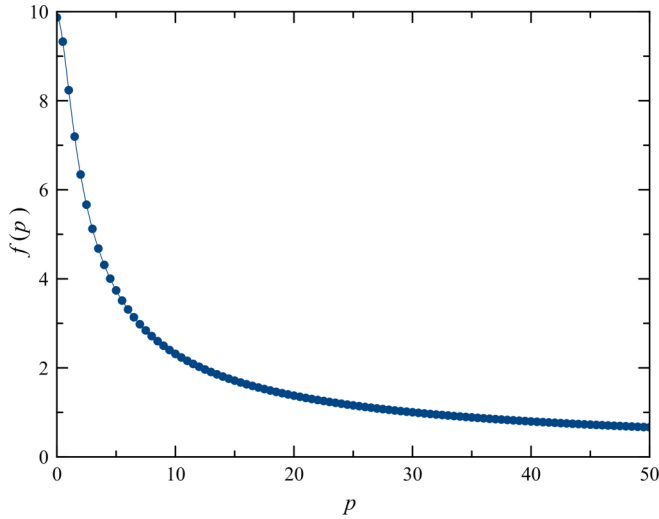


FIG. 2. The plot of the function  $f(p)$  given by Eq. (24).

here. The function  $f(p)$  plotted numerically is shown in Fig. 2. Its asymptotic behavior can be computed analytically:

$$S_z = \left(\frac{\lambda}{a}\right)^2 \begin{cases} \pi^2, & d = 0 \\ 16\pi(\lambda/d)^2 \ln(d/\lambda), & d \gg \lambda. \end{cases} \quad (25)$$

Numerical evaluation gives a more accurate but close result,  $\ln(1.1d/\lambda)$ , for the logarithmic cutoff in the case of  $d \gg \lambda$ .

According to Fig. 2 and Eqs. (22) and (25), at a fixed  $\lambda$  the magnetic moment of the biskyrmion rapidly decreases on increasing  $d$ . One should notice, however, that in this limit the total spin of the biskyrmion can be written as

$$S_z = 8\pi \left(\frac{\tilde{\lambda}}{a}\right)^2 \ln\left(\frac{1.05d}{\tilde{\lambda}}\right) \quad (26)$$

in terms of the effective size  $\tilde{\lambda} = \lambda^2/d \ll \lambda$  of the  $Q = 1$  skyrmion in a biskyrmion. Note that the magnetic moment of an isolated  $Q = 1$  skyrmion is given by [43]

$$S_z^{(1)} = 4\pi \left(\frac{\tilde{\lambda}}{a}\right)^2 \ln\left(\frac{\Lambda}{\tilde{\lambda}}\right), \quad (27)$$

where  $\Lambda$  is a long-distance cutoff determined by the lateral dimension of the film,  $L$ , or by  $\delta_H = \sqrt{J/H}$ , whichever is shorter. Thus, by order of magnitude,  $S_z$  remains the same regardless of the separation of  $Q = 1$  skyrmions in the biskyrmion and similar to the magnetic moment of an isolated  $Q = 1$  skyrmion. As we shall see the energy minimum of a biskyrmion in a real magnetic film is realized at  $d \sim \lambda$ . In this case  $S_z \propto d^2 \sim \lambda^2$ , that is, the magnetic moment is proportional to the area occupied by the biskyrmion.

### C. Lattice-discreteness correction to the energy

The scale invariance of the skyrmion energy is broken by the discreteness of the lattice. The exchange energy of the atomic spins considered as classical spin vectors with  $|\mathbf{s}_i| = 1$  has the form

$$\mathcal{H}_{\text{ex}} = -\frac{1}{2} \sum_{ij} J_{ij} \mathbf{s}_i \cdot \mathbf{s}_j, \quad (28)$$

where  $J_{ij} = J$  for the nearest neighbors and zero otherwise. We use the simple cubic lattice. The corresponding correction to the energy can be obtained by calculating this lattice sum using the BP solution. For  $\lambda \gtrsim a$ , expanding the dot products to the lowest second order in spatial derivatives of the spin field, one obtains the well-known result

$$E_{\text{ex}} = \frac{J}{2} \int dx dy [(\partial_x \mathbf{s})^2 + (\partial_y \mathbf{s})^2]$$

that is equivalent to Eq. (1) and leads to Eq. (4). Expansion to the fourth order yields the energy correction

$$\delta E_{\text{ex}} = -\frac{Ja^2}{24} \int dx dy [(\partial_x^2 \mathbf{s})^2 + (\partial_y^2 \mathbf{s})^2]. \quad (29)$$

For a singled-centered skyrmion with an arbitrary  $Q$ , substituting Eqs. (15) into Eq. (29), we obtain with the help of computer algebra

$$\delta E_{\text{ex}} = -\frac{\pi^2 J}{3} \frac{Q^2 - 1}{\sin(\pi/|Q|)} \left(\frac{a}{\lambda}\right)^2. \quad (30)$$

The previously obtained result in Ref. [25] for  $Q = \pm 1$ ,

$$\delta E_{\text{ex}} = -\frac{2\pi J}{3} \left(\frac{a}{\lambda}\right)^2, \quad (31)$$

follows from this formula in the limit of  $|Q| \rightarrow 1$ .

## III. BISKYRMIONS IN A MAGNETIC FILM WITH PERPENDICULAR MAGNETIC ANISOTROPY

### A. Lattice model and dipolar field

In the numerical work, we study the lattice model of a ferromagnetic film of finite thickness with the energy given by the sum over lattice sites  $i, j$ :

$$\mathcal{H} = \mathcal{H}_{\text{ex}} - H \sum_i s_{iz} - \frac{D}{2} \sum_i s_{iz}^2 - \frac{E_D}{2} \sum_{ij} \Phi_{ij,\alpha\beta} s_{i\alpha} s_{j\beta}. \quad (32)$$

Here  $\mathcal{H}_{\text{ex}}$  is given by Eq. (28),  $D$  is the easy-axis PMA constant, and  $H \equiv g\mu_B SB$ , with  $S$  being the value of the atomic spin and  $B$  being the induction of the applied magnetic field. In the DDI part of the energy,

$$\Phi_{ij,\alpha\beta} \equiv a^3 r_{ij}^{-5} (3r_{ij,\alpha} r_{ij,\beta} - \delta_{\alpha\beta} r_{ij}^2), \quad (33)$$

where  $\mathbf{r}_{ij} \equiv \mathbf{r}_i - \mathbf{r}_j$  is the displacement vector between the lattice sites and  $\alpha, \beta = x, y, z$  denote Cartesian components. The parameter  $E_D = \mu_0 M_0^2 a^3 / (4\pi)$  defines the strength of the DDI, with  $M_0 = g\mu_B S/a^3$  being the magnetization for our lattice model and  $\mu_0$  being the magnetic permeability of vacuum.

The ratio of the PMI and DDI is given by the dimensionless parameter  $\beta \equiv D/(4\pi E_D)$ . For  $\beta > 1$ , the energy of the uniform state with spins directed along the  $z$  axis is lower than that of the state with spins lying in the film's plane. For  $\beta < 1$ , the state with spins in the plane has a lower energy. The most interesting practical case is  $\beta \sim 1$  realized in many materials in which there is a considerable compensation of the effects of the PMA and DDI.

In most materials, the exchange interaction is much stronger than all other interactions of the spins. Consequently,

in a centrosymmetric system with magnetic anisotropy and nonsingular defects, such as skyrmions, the magnetization can only smoothly rotate on a large spatial scale gauged by two lengths: the domain-wall width,  $\delta = a\sqrt{J/D} \gg a$ , and another length,  $\delta_H = a\sqrt{J/H} \gg a$ , generated by the field. To describe such nonuniform spin states, one needs to consider a system with macroscopically large number of spins. In the lattice model, this can lead to impractically large computation times. Besides, the systems with interactions that are weak compared to the ferromagnetic exchange are magnetically soft because the energy of the nonuniform structures per spin is small. This makes the convergence of the energy-minimization routine very slow. The good news is that in such a case the atomic-scale spatial resolution is excessive.

To speed up the computation for structures that are much larger than the atomic spacing  $a$ , one can rescale the problem to another lattice constant  $b > a$  by first rewriting the energy in the continuous approximation and then discretizing it again. The rescaled model with the parameters

$$J' = \frac{b}{a}J, \quad H' = \frac{b^3}{a^3}H, \quad D' = \frac{b^3}{a^3}D, \quad E'_D = \frac{b^3}{a^3}E_D \quad (34)$$

has smaller number of mesh points  $N'_\alpha = (a/b)N_\alpha$  and smaller mismatch between  $J$  and other parameters. This provides faster convergence. After the computation with the rescaled model is completed, one obtains the results for the original system by rescaling the parameters back. Note that the domain-wall width and the field-related length are the same in the original and rescaled models:

$$\delta' = b\sqrt{\frac{J'}{D'}} = a\sqrt{\frac{J}{D}} = \delta, \quad \delta'_H = b\sqrt{\frac{J'}{H'}} = a\sqrt{\frac{J}{H}} = \delta_H. \quad (35)$$

The same is valid for all spatial structures such as magnetic bubbles, etc. The above-mentioned rescaling is only important for the study of films of large lateral dimensions. In a confined geometry, such as, e.g., nanotracks, one can perform computation at the atomic level.

The use of strong anisotropy and strong DDI allows one to work with a relatively small system and to have a reasonably fast convergence [37]. In this case, however, the shape of the topological defects is closer to that of the thin-wall skyrmion bubbles than to the BP skyrmions. To obtain the latter one has to work with the skyrmion size  $\lambda$  satisfying  $a \lesssim \lambda \lesssim \delta$  that requires a smaller anisotropy constant. To investigate biskyrmions, which is the purpose of this paper, we use  $D/J = 0.001$ . This requires a large system size,  $N_x \times N_y = 1000 \times 1000$ , and results in longer computation times.

An important parameter controlling the DDI is the film thickness represented by  $N_z$  in the units of the atomic spacing  $a$ . For thin films that are studied here, the magnetization inside the film is nearly constant along the direction perpendicular to the film. Thus one can make the problem effectively 2D by introducing the effective DDI between the columns of parallel spins, considered as effective spins of the 2D model. This greatly speeds up the computation. To this end, for the simple cubic lattice, one can write the dipolar coupling, Eq. (33), as  $\Phi_{i,j,\alpha\beta} = \phi_{\alpha\beta}(n_x, n_y, n_z)$ , where  $n_x \equiv i_x - j_x$  etc., are the

distances on the lattice and

$$\phi_{\alpha\beta}(n_x, n_y, n_z) = \frac{3n_\alpha n_\beta - \delta_{\alpha\beta}(n_x^2 + n_y^2 + n_z^2)}{(n_x^2 + n_y^2 + n_z^2)^{5/2}}. \quad (36)$$

The effective DDI is defined by

$$\bar{\phi}_{\alpha\beta}(n_x, n_y) = \frac{1}{N_z} \sum_{i_z, j_z=1}^{N_z} \phi_{\alpha\beta}(n_x, n_y, i_z - j_z). \quad (37)$$

Using the symmetry, one can express this result in the form with only one summation,

$$\begin{aligned} \bar{\phi}_{\alpha\beta}(n_x, n_y) &= \phi_{\alpha\beta}(n_x, n_y, 0) \\ &+ \frac{2}{N_z} \sum_{n_z=1}^{N_z-1} (N_z - n_z) \phi_{\alpha\beta}(n_x, n_y, n_z), \end{aligned} \quad (38)$$

that is used in the computations.

The effective DDI (that can be precomputed) has different forms in different ranges of the distance  $r$ . At  $r \gtrsim aN_z$ , it scales as the interaction of magnetic dipoles  $1/r^3$ , while at  $r \lesssim aN_z$  it goes as  $1/r$  that corresponds to the interaction of magnetic charges at the surface of the film. Numerical results in Fig. 3 show that at large distances the effective DDI is stronger in films of finite thickness than in pure 2D systems. This has an important effect on the stability of biskyrmions.

In the computations, the dipolar field from the downward spins outside the system was added to obtain the results that are valid for an infinite system. This field was computed as the field of the plate of a very large size magnetized downward plus the dipolar field created by the finite system under the consideration magnetized upward.

## B. Energy landscape of rigid-shape biskyrmions

Interactions other than exchange deform BP skyrmions and biskyrmions. As a result, the exchange energy increases. In the numerical work, this increase provides the measure of the shape distortion. Also, one can consider the energy  $\Delta E$  of the state with skyrmions with respect to that of the uniform state with all spins down. This energy is smaller than  $4\pi J|Q|$  due to the contributions of the PMA and DDI.

We start with exploring the energy landscape,  $E(\lambda, d)$ , in the presence of biskyrmions, assuming the rigid BP shape given by Eqs. (9)–(11) and numerically calculating the energy with the help of Eq. (32). This is valid when the exchange is much greater than all other interactions and when the biskyrmion size is small compared to the domain wall width:  $\lambda, d \lesssim \delta$ . In fact, it is more convenient to parametrize  $\lambda$  as  $\lambda^2 = \tilde{\lambda}(\tilde{\lambda} + d)$ , where  $\tilde{\lambda}$  is the actual size of an individual  $Q = 1$  skyrmion in the limit of a large separation  $d$ .

Whereas in the pure exchange model the energy of biskyrmions is independent of  $\lambda$  and  $d$ , other interactions (here PMA, DDI, and Zeeman), with the applied field  $H$  as a control parameter, break this invariance of the skyrmion energy and select the values of  $\lambda$  and  $d$  that provide the energy minimum. The energy minimum of the topological defect with  $Q = 2$  always corresponds to a biskyrmion with  $d \neq 0$ .

To the contrary, we find that for a biantiskymion, the energy always has a minimum at  $d = 0$ , thus, there should be only

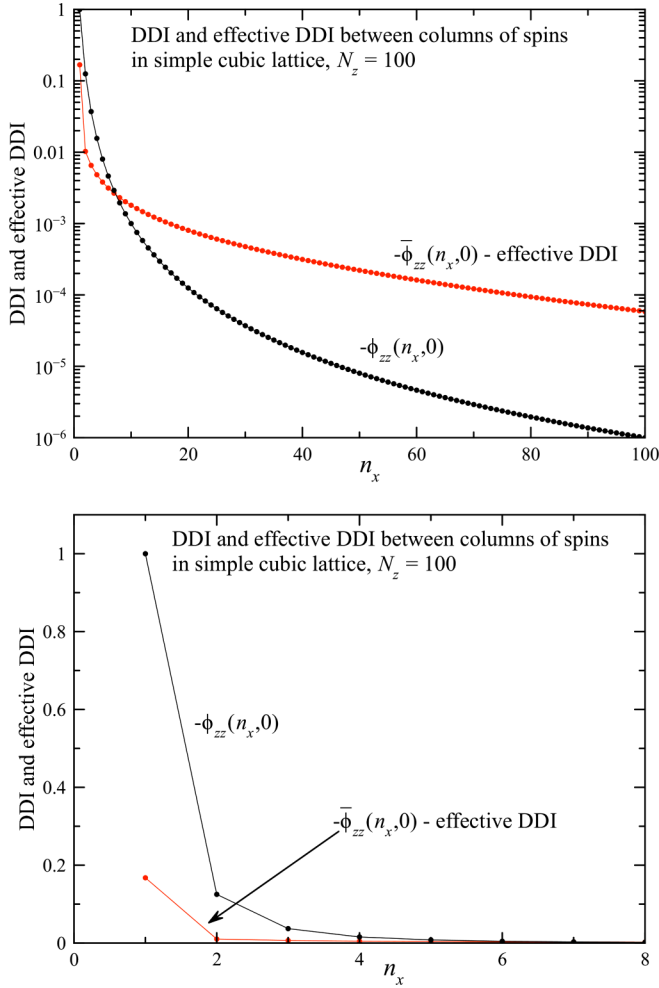


FIG. 3. DDI and effective DDI between columns of spins in a simple cubic lattice for the film thickness  $N_z = 100$ . Upper panel: Logarithmic scale. Lower panel: Linear scale at short distances.

$d = 0$  single-centered antiskyrmions with  $Q = -2$ . This confirms the findings of Ref. [37], see Fig. 9 that shows different kinds of magnetic bubbles obtained by the relaxation from a random spin state: All objects with  $Q = -2$  are spatially symmetric antiskyrmions, whereas all objects with  $Q = 2$  have a finite separation,  $d \neq 0$ .

Figure 4 (upper panel) shows an example of the biskyrmion energy landscape for the system of size  $N_x \times N_y \times N_z = 1000 \times 1000 \times 100$  for which most of the computations have been done. We used  $D/J = 0.001$  and  $\beta = 1$ . For  $H/J = -0.00015$ , there is a local energy minimum at  $\lambda/a = 27.1$  and  $d/a = 41.5$ . The difference  $\Delta E$  from the energy of the uniformly magnetized state with spins down is given in the units of  $4\pi J$ . For a weakly distorted BP biskyrmion it is close to 2. As the parameter  $\lambda$  decreases, the energy goes down due the lattice-discreteness correction, see Sec. II C. On the other hand, for the biantiskyrmion shown in Fig. 5 (upper panel), for the same parameters as above, there is no energy minimum at all, see lower panel in Fig. 4. Thus the biantiskyrmion evolves to a  $Q = -2$  antiskyrmion shown in Fig. 5 (lower panel). It should be noted that the computed energy landscape is the

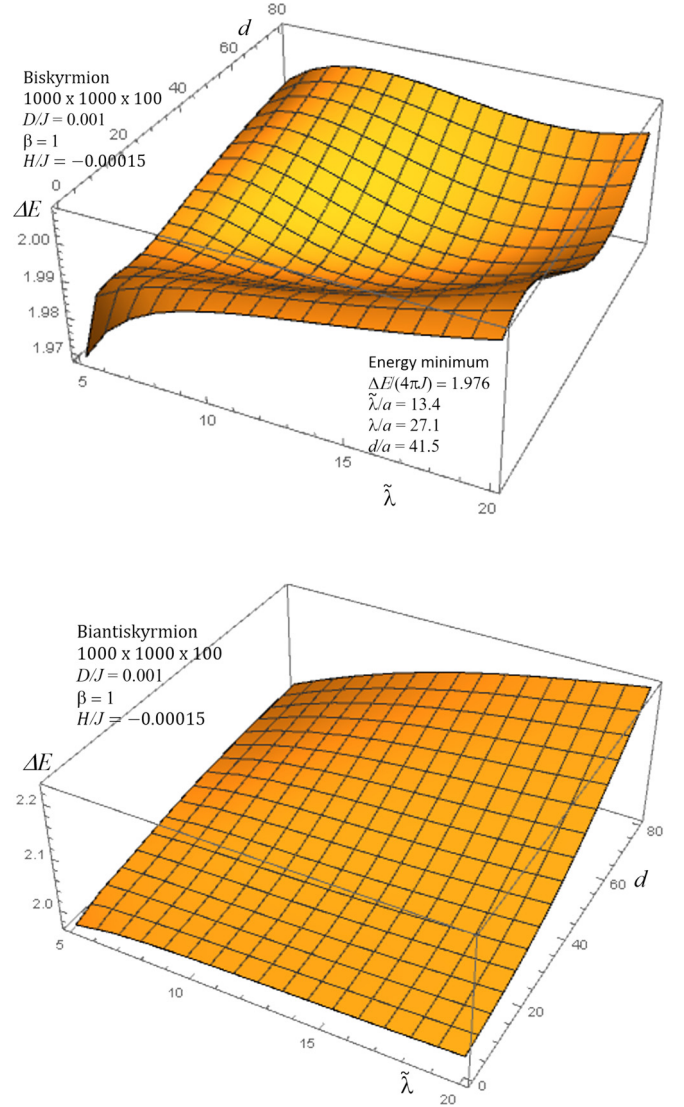


FIG. 4. The energy landscape of a Belavin-Polyakov biskyrmion (upper panel) and biantiskyrmion (lower panel). The biskyrmion has a local energy minimum at a finite separation,  $d > 0$ , while the biantiskyrmion for the same parameters has no energy minimum at all.

same for  $\phi = 0$  and  $\phi = \pi/2$ . For smaller  $|H|$ , there is an energy minimum of the biantiskyrmion at  $d = 0$  and  $\lambda > 0$ .

Whereas the rigid biskyrmion approximation provides a good qualitative description, it is not completely accurate since the balance of different interactions is very subtle and small deformations of the shape have a significant effect on the energy. More accurate results can be obtained by the numerical energy minimization described in the next section.

### C. Numerical energy minimization and results

In this section, we compute minimum-energy configurations of spins. The numerical method [44] combines sequential rotations of spins  $\mathbf{s}_i$  toward the direction of the local effective field,  $\mathbf{H}_{\text{eff},i} = -\partial\mathcal{H}/\partial\mathbf{s}_i$ , with the probability  $\alpha$ , and the energy-conserving spin flips (so-called *overrelaxation*),  $\mathbf{s}_i \rightarrow 2(\mathbf{s}_i \cdot \mathbf{H}_{\text{eff},i})\mathbf{H}_{\text{eff},i}/H_{\text{eff},i}^2 - \mathbf{s}_i$ , with the probability  $1 - \alpha$ .

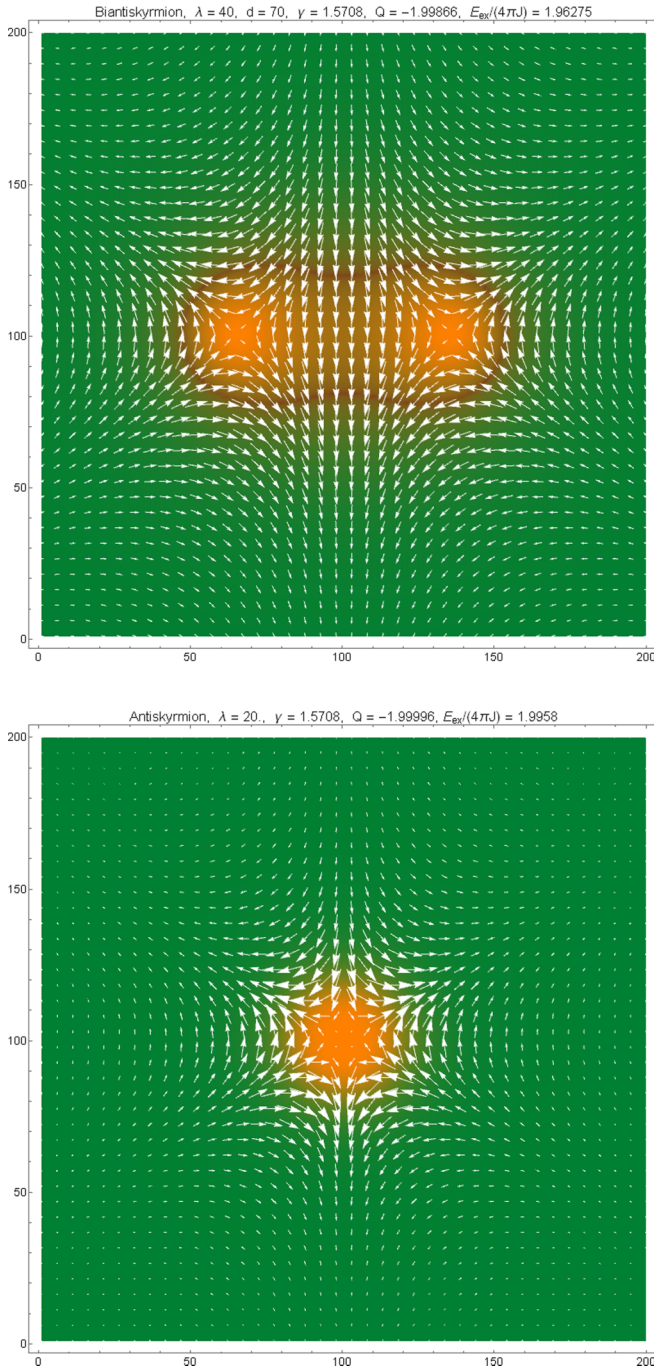


FIG. 5. Upper panel: Spin field in a  $Q = -2$  BP biantiskyrmion ( $d > 0$ ). Lower panel: Spin field in a  $Q = -2$  BP antiskyrmion ( $d = 0$ ). In the presence of DDI, PMA, and the applied magnetic field, the initial state with  $d > 0$  in the course of relaxation evolves to the minimal-energy state with  $d = 0$ .

The parameter  $\alpha$  plays the role of the effective relaxation constant. We mainly use the value  $\alpha = 0.03$  that provides the overall fastest convergence.

The dipolar part of the effective field takes the longest time to compute. The method uses fast Fourier transform (FFT) in the whole sample as one program step. Since the dipolar field is much weaker than the exchange, several cycles of spin alignment can be performed before the dipolar field is

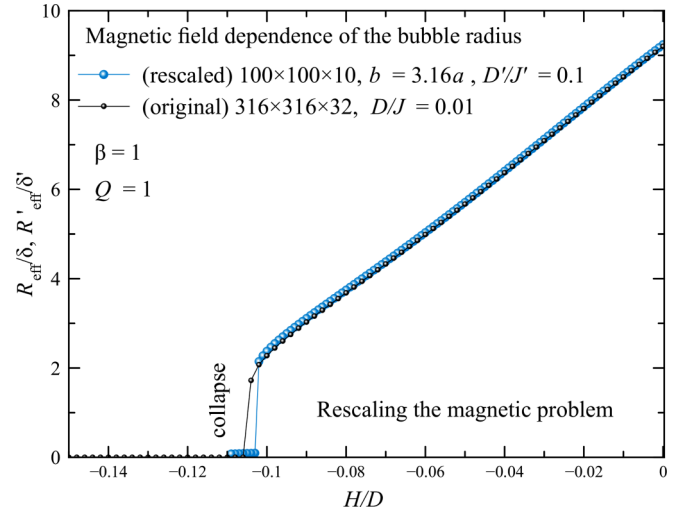


FIG. 6. Magnetic-field dependence of the effective radius of a stable skyrmion bubble for the “original” and rescaled models.

updated, which increases the computation speed. The total charge  $Q$  of the topological defect has been computed numerically using the lattice-discretized version of Eq. (2).

Computations were performed with Wolfram Mathematica using compilation. Most of the numerical work has been done on the 20-core Dell Precision T7610 Workstation. The FFT for computing the DDI was performed via Mathematica’s function ListConvolve that implicitly uses many processor cores. For this reason, no explicit parallelization was done in our program. However, we have been able to run several independent computations at the same time.

To demonstrate how well our rescaling method given by Eqs. (34) works, we have computed the effective radius  $R_{\text{eff}}$  of topological defects with  $Q = 1$ , defined as  $\pi R_{\text{eff}}^2 = S_z/2$ , where  $S_z$  is the total spin of the bubble defined by  $S_z = \int dx dy [s_z(x, y) + 1]$ . The “original” system is a grid of  $316 \times 316 \times 32$  spins with  $D/J = 0.01$  and the lattice constant  $a$ . The rescaled system is a grid of  $100 \times 100 \times 10$  spins with  $D'/J' = 0.1$  and the lattice constant  $b = \sqrt{10}a = 3.16a$ . In both cases,  $\beta = 1$ . Figure 6 shows a perfect agreement between  $R_{\text{eff}}$  and  $R'_{\text{eff}}$ . (Note that  $\delta' = \delta$  thus practically  $R'_{\text{eff}} = R_{\text{eff}}$ ) in the plot.

Subsequently, we performed the energy minimization for biskyrmions with  $Q = 2$  in a system with  $N_x \times N_y \times N_z = 1000 \times 1000 \times 100$ ,  $D/J = 0.001$ , and  $\beta = 1$  at different values of the applied field  $H$ . The separation  $d$  was found numerically as the distance between the maxima of  $s_z$  in the biskyrmion. Then  $\lambda$  was extracted with the help of Eq. (12) using the numerically found saddle-point value of  $s_z$ .

In Fig. 7, one can see that there is always a finite separation,  $d > 0$ , in the biskyrmion. For stronger fields, the biskyrmion is smaller and closer to the BP shape, as the energies  $E_{\text{ex}}$  and  $\Delta E$  are close to  $8\pi J$ . Biskyrmions collapse as the field reaches the stability threshold. With decreasing the magnitude of field the biskyrmion is expanding, gradually transforming into a thin-wall bubble. The ratio  $d/\lambda$  changes from 1.5 on the left side of Fig. 7 to 1.1 on its right side. The transition from BP biskyrmions to biskyrmion bubbles can be seen in a significant deviation of energy from  $E/(4\pi J) = 2$ . As the

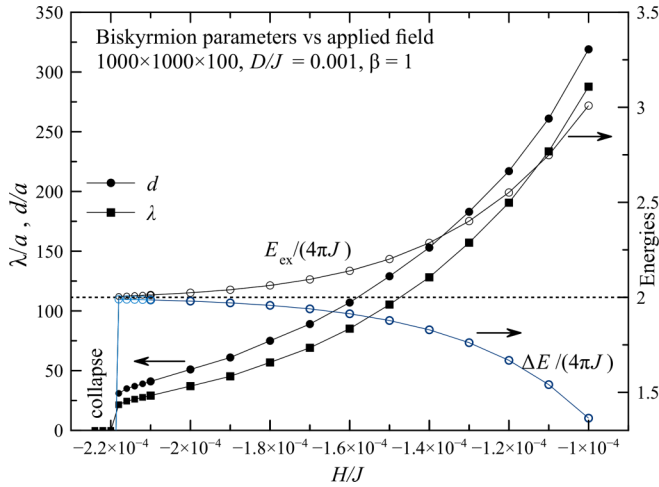


FIG. 7. Magnetic field dependencies of the parameters  $\lambda$  and  $d$  of stable biskyrmions in a film of thickness  $N_z = 100$  with  $D/J = 0.001$  and  $\beta = 1$ . Exchange energy  $E_{\text{ex}}$  and the total energy  $\Delta E$  (with respect to the uniformly magnetized spins with spins down) are shown on the right y axis. For stronger fields, the biskyrmion is smaller and close to the BP biskyrmion, as shown by the energies.

field strength further decreases, the bubble loses its circular shape and transforms into a laminar domain.

Typical spin configurations of biskyrmions are illustrated (zoomed) in Fig. 8 that provides more details as compared to Fig. 1. The in-plane spin components in a BP biskyrmion shown in the upper panel of Fig. 8 decay as  $1/r^2$  in accordance with Eqs. (9) and (13). On the contrary, in a biskyrmion bubble shown in the lower panel of Fig. 8 the in-plane spin components decay exponentially and are hardly visible away from the bubble. For topological defects with  $Q = -2$  (antiskyrmions) no finite separation  $d$  was detected in our computations.

Next we performed computations for a similar model with a stronger DDI,  $\beta = 0.5$ . The DDI in excess of the PMA forces the spins into the film's plane, which suppresses skyrmions. To prevent this from happening, a stronger negative magnetic field has to be applied. The results in Fig. 9 show a larger separation,  $d/\lambda \gtrsim 2$ , and the shape close to the BP shape as  $E_{\text{ex}}/(4\pi J)$  is rather close to 2. On the right side of the figure, the instability of the uniform state with spins down occurs on decreasing the field's strength.

For the model in which PMA is stronger than DDI,  $\beta > 1$ , no stable skyrmions or biskyrmions were found as they were collapsing even at  $H = 0$ . The topological structures can be stabilized by the negative magnetic field in the range  $\beta^* < \beta < 1$  that depends on the film's thickness  $N_z$ . Numerical studies show that the range of  $\beta$  narrows down for thin films. In the latter, the effect of the DDI is similar to that of the easy-plane PMA, so one can introduce the effective anisotropy that includes both PMA and DDI,  $\tilde{D} = D(1 - 1/\beta)$ . This effective anisotropy changes its sign at  $\beta = 1$ . This results in the extremely weak distortion of the BP shape of biskyrmions and extremely small controlling fields  $H$ . However, the model with a single effective anisotropy cannot support stable topological defects, including skyrmions and biskyrmions, at any  $\beta \neq 1$ . Since in real materials  $\beta$  cannot be tuned, very thin

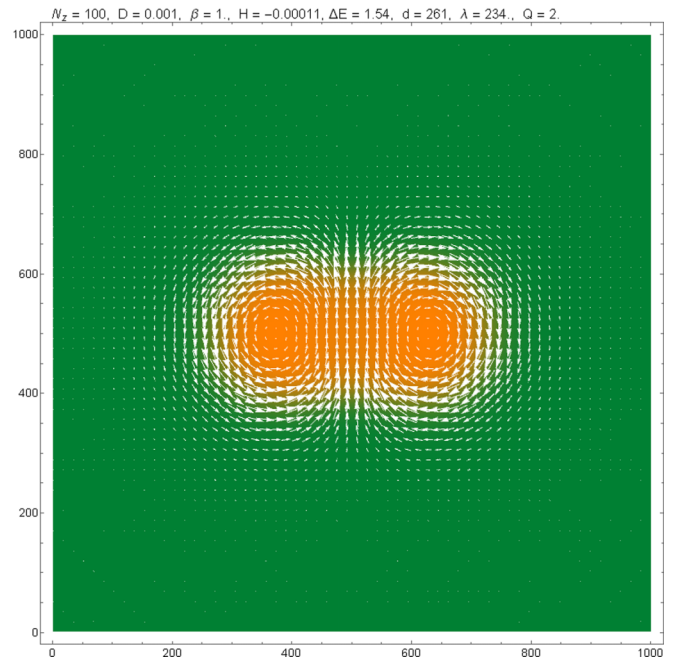
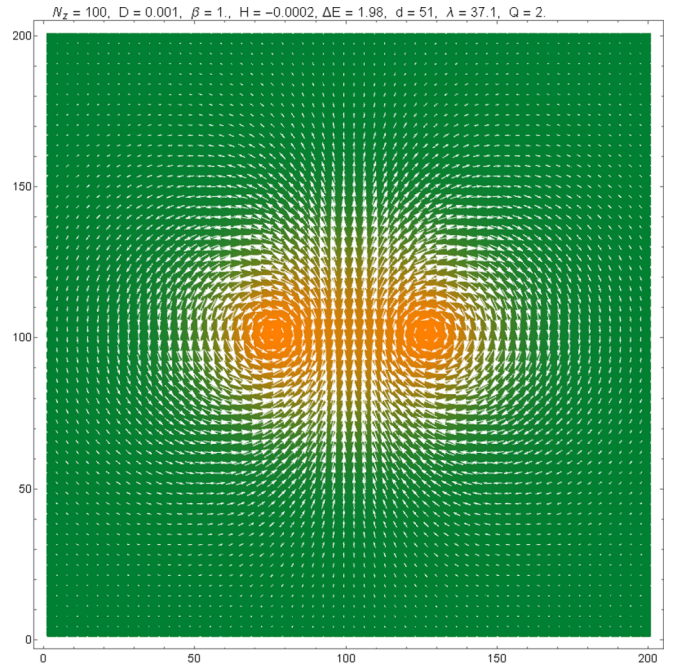


FIG. 8. Computer-generated images of the spin field in a stable BP biskyrmion (upper panel) and a biskyrmion bubble (lower panel) numerical solutions of the centrosymmetric Heisenberg lattice model with the ferromagnetic exchange, DDI, PMA, and external field. The values of parameters are written above the figures. Orange/green color indicates positive/negative  $z$  components of the spin field. The in-plane spin components are shown as white arrows.

nonchiral films with no DMI are not a good medium for the skyrmions. To the contrary, for thicker films, competition of the short-range PMA and long-range ( $\sim 1/r$ ) DDI creates a range of  $\beta$  in which skyrmions and biskyrmions can exist.

In particular, for  $N_z = 20$  with  $D/J = 0.001$ , stable biskyrmions were found only for  $\beta = 1$ . The results in Fig. 10

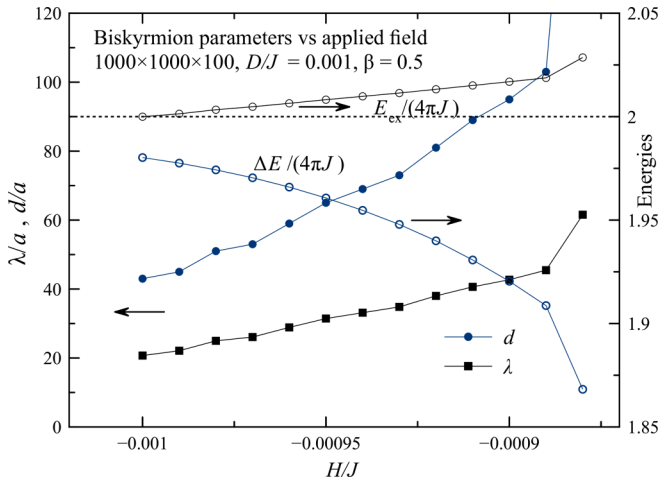


FIG. 9. Magnetic field dependencies of the parameters  $\lambda$  and  $d$  of stable biskyrmions in a film of thickness  $N_z = 100$  with  $D/J = 0.001$  and  $\beta = 0.5$ .

show very weakly distorted BP biskyrmions with practically the same ratio  $d/\lambda = 1.62$  in the whole range of a very weak field  $H$ . For  $\beta = 0.5$  and even for  $\beta = 0.75$ , either the skyrmions collapse if the negative field is too strong or the background spin-down state becomes unstable if the negative field is too weak. For the system of  $500 \times 500 \times 10$  spins, biskyrmions were still found at  $\beta = 1$  but the range of  $H$  was much narrower. One can see that here the exchange energy is much closer to 2 than for  $N_z = 20$ , thus the shape of the biskyrmion is much closer to the BP shape. For  $H/J < -3.8 \times 10^{-5}$  the biskyrmion collapses. For  $H/J > -2 \times 10^{-5}$ , the spin-down background becomes unstable.

Computations on the  $500 \times 500$  monolayer found no biskyrmions at all even for  $\beta = 1$ . Initial states in the form of biskyrmions evolve into states with separate skyrmions far away from each other that exist in an extremely narrow region of  $H$ .

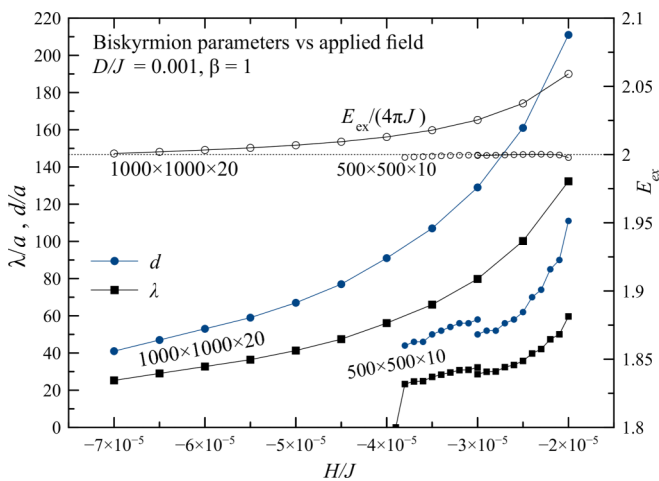


FIG. 10. Magnetic-field dependencies of the parameters  $\lambda$  and  $d$  of stable biskyrmions (left axis) and the exchange energy (right axis) in films of thickness  $N_z = 20$  and  $10$  with  $D/J = 0.001$  and  $\beta = 1$ .

The bottom line of this investigation is that biskyrmions should be searched for in sufficiently thick films, such as  $N_z = 100$  for  $D/J = 0.001$ . For other values of the PMA, the scaling of Eqs. (34) can be used. For a stronger PMA, biskyrmions can be supported by thinner films.

#### IV. DISCUSSION

We have studied biskyrmions in nonchiral ferromagnetic films of finite thickness with PMA with account of DDI, and discreteness of the atomic lattice. In agreement with experimental findings [35,36] we have found that biskyrmions are stable above a certain threshold in the film thickness. In films of insufficient thickness, (e.g., with the number of the atomic layers  $N_z = 10$  for  $D/J = 0.001$ , stable biskyrmions exist only at  $\beta = \text{PMA}/\text{DDI} = 1$ , when the DDI nearly compensates the effect of the PMA. Since this condition is impossible to satisfy in practice, we conclude that stable biskyrmions do not exist in thin nonchiral magnetic films that contain just a few atomic layers. For the monolayer,  $N_z = 1$ , no biskyrmions at all were found.

In thicker films (with, e.g.,  $N_z \sim 100$  for  $D/J = 0.001$  and thus  $\delta/a \lesssim N_z$ ), stable biskyrmions exist within a finite range of  $\beta$  below  $\beta = 1$ . For stronger stabilizing fields, smaller biskyrmions of sizes  $\lambda \lesssim d \lesssim \delta$  and the shape close to that provided by the BP 2D exchange model, Eqs. (9)–(11), have been observed in our numerical studies. Their energy is close to  $8\pi J$ . Such BP biskyrmions collapse at a critical value of the stabilizing field. In the opposite limit, when the magnitude of the stabilizing field decreases, the BP biskyrmion transforms into a bigger thin-wall biskyrmion bubble. Regardless of the film thickness and other parameters, we did not find any stable biantiskyrmions with  $d > 0$ .

The study presented here has focused on the stability of individual biskyrmions. Biskyrmions observed in experiments [35,36] formed distorted triangular lattices. They were obtained from labyrinth domains on increasing the magnetic field in a manner similar to how lattices of  $Q = 1$  skyrmions have been observed. While our numerical method easily generated lattices of  $Q = 1$  skyrmions in the films with DMI, numerical generation of stable biskyrmion lattices in centrosymmetric 2D systems remains a challenging problem.

In our computations, stability of a single biskyrmion required an external field while the biskyrmion lattice has been observed even in a zero field [35]. This means that a sufficiently dense biskyrmion lattice minimizes the sum of the exchange, DDI, and PMA energies at  $H = 0$ , similarly to what happens in the domain state.

For practical applications, one has to be able to generate and manipulate individual biskyrmions. It has been demonstrated that skyrmions can be created, annihilated, and moved by current-induced spin-orbit torques [6,45,46]. Individual  $Q = 1$  skyrmion bubbles have been generated by pushing elongated magnetic domains through a constriction using an in-plane current [5,47]. These methods may not be suited for creating biskyrmions.

It has been shown that small skyrmions can be written and deleted in a controlled fashion with local spin-polarized currents from a scanning tunneling microscope [48]. It has been

also demonstrated that light-induced heat pulses of different duration and energy can write skyrmions in a magnetic film in a broad range of temperatures and magnetic fields [49]. These methods can be better suited for creating biskymions if experimentalists find the way of using a scanning tunneling microscope with a double tip or heat pulses of the shape resembling biskymions.

Recently, it has been experimentally demonstrated and confirmed through micromagnetic computations that stripe domains in a film can be cut into  $Q = 1$  skyrmions by the magnetic field of the tip of a scanning magnetic force microscope (MFM) [50]. Writing individual  $Q = 1$  skyrmions by the MFM tip has been studied theoretically in Ref. [42]. One can also use for that purpose magnetic nanoparticles of the kind used in nanocantilevers for mechanical magnetometry [51].

A simple modification of the above method, tailored to biskymions, may be developed by using a double MFM tip consisting of two single tips in close proximity to each other, or a nanocantilever with two magnetic nanoparticles next to each other. We have tested this numerically in the same manner as is described in detail in Ref. [42]. A biskymion

created this way in the numerical experiment relaxes to the equilibrium size and shape determined by the parameters of the film.

Since biskymions carry magnetic moments similar to those of  $Q = 1$  skyrmions, they can be utilized in a similar way for data storage and information processing. The lack of the rotational symmetry in a biskymion makes its orientation another useful parameter in addition to the magnetic moment. It can open other functionalities in manipulating such information carriers as well. For example, the magnitude of the force exerted on a biskymion by the spin polarized current would depend on the direction of the current.

*Note added.* After this paper was submitted, more articles have appeared that provided further experimental and numerical evidence of stable biskymions in centrosymmetric magnetic materials [52–54].

#### ACKNOWLEDGMENT

This work has been supported by Grant No. OSR-2016-CRG5-2977 from King Abdullah University of Science and Technology.

- 
- [1] N. Nagaosa and Y. Tokura, Topological properties and dynamics of magnetic skyrmions, *Nat. Nanotech.* **8**, 899 (2013).
  - [2] X. Zhang, M. Ezawa, and Y. Zhou, Magnetic skyrmion logic gates: Conversion, duplication and merging of skyrmions, *Sci. Rep.* **5**, 9400 (2015).
  - [3] G. Finocchio, F. Büttner, R. Tomasello, M. Carpentieri, and M. Klaui, Magnetic skyrmions: From fundamental to applications, *J. Phys. D* **49**, 423001 (2016).
  - [4] A. O. Leonov, T. L. Monchesky, N. Romming, A. Kubetzka, A. N. Bogdanov, and R. Wiesendanger, The properties of isolated chiral skyrmions in thin magnetic films, *New J. Phys.* **18**, 065003 (2016).
  - [5] W. Jiang, G. Chen, K. Liu, J. Zang, S. G. E. te Velthuis, and A. Hoffmann, Skyrmions in magnetic multilayers, *Phys. Rep.* **704**, 1 (2017).
  - [6] A. Fert, N. Reyren, and V. Cros, Magnetic skyrmions: Advances in physics and potential applications, *Nat. Rev. Mater.* **2**, 17031 (2017).
  - [7] T. H. R. Skyrme, A non-linear theory of strong interactions, *Proc. R. Soc. A* **247**, 260 (1958).
  - [8] A. M. Polyakov, *Gauge Fields and Strings* (Harwood Academic Publishers, New York, 1987).
  - [9] N. Manton and P. Sutcliffe, *Topological Solitons* (Cambridge University Press, Cambridge, England, 2004).
  - [10] A. A. Belavin and A. M. Polyakov, Metastable states of two-dimensional isotropic ferromagnets, *Pis'ma Zh. Eksp. Teor. Fiz.* **22**, 503 (1975) [*JETP Lett.* **22**, 245 (1975)].
  - [11] E. M. Chudnovsky and J. Tejada, *Lectures on Magnetism* (Rinton Press, Princeton, NJ, 2006).
  - [12] *The Multifaceted Skyrmion*, edited by G. E. Brown and M. Rho (World Scientific, Singapore, 2010).
  - [13] U. Al'Khawaja and H. T. C. Stoof, Skyrmions in a ferromagnetic Bose-Einstein condensate, *Nature* **411**, 918 (2001).
  - [14] S. L. Sondhi, A. Karlhede, S. A. Kivelson, and E. H. Rezayi, Skyrmions and the crossover from the integer to fractional quantum Hall effect at small Zeeman energies, *Phys. Rev. B* **47**, 16419 (1993).
  - [15] M. Stone, Magnus force on skyrmions in ferromagnets and quantum Hall systems, *Phys. Rev. B* **53**, 16573 (1996).
  - [16] J. Ye, Y. B. Kim, A. J. Millis, B. I. Shraiman, P. Majumdar, and Z. Tesanovic, Berry Phase Theory of the Anomalous Hall Effect: Application to Colossal Magnetoresistance Manganites, *Phys. Rev. Lett.* **83**, 3737 (1999).
  - [17] D. C. Wright and N. D. Mermin, Crystalline liquids: The blue phases, *Rev. Mod. Phys.* **61**, 385 (1989).
  - [18] A. P. Malozemoff and J. C. Slonczewski, *Magnetic Domain Walls in Bubble Materials* (Academic Press, New York, 1979).
  - [19] T. H. O'Dell, *Ferromagnetodynamics: The Dynamics of Magnetic Bubbles, Domains, and Domain Walls* (Wiley, New York, 1981).
  - [20] B. A. Ivanov, A. Y. Merkulov, V. A. Stepanovich, and C. E. Zaspel, Finite energy solitons in highly anisotropic two dimensional ferromagnets, *Phys. Rev. B* **74**, 224422 (2006).
  - [21] E. G. Galkina, E. V. Kirichenko, B. A. Ivanov, and V. A. Stepanovich, Stable topological textures in a classical two-dimensional Heisenberg model, *Phys. Rev. B* **79**, 134439 (2009).
  - [22] C. Moutafis, S. Komineas, and J. A. C. Bland, Dynamics and switching processes for magnetic bubbles in nanoelements, *Phys. Rev. B* **79**, 224429 (2009).
  - [23] M. Ezawa, Giant Skyrmions Stabilized by Dipole-Dipole Interactions in thin Ferromagnetic Films, *Phys. Rev. Lett.* **105**, 197202 (2010).
  - [24] I. Makhfudz, B. Krüger, and O. Tchernyshyov, Inertia and Chiral Edge Modes of a Skyrmion Magnetic Bubble, *Phys. Rev. Lett.* **109**, 217201 (2012).

- [25] L. Cai, E. M. Chudnovsky, and D. A. Garanin, Collapse of skyrmions in two-dimensional ferromagnets and antiferromagnets, *Phys. Rev. B* **86**, 024429 (2012).
- [26] E. M. Chudnovsky and D. A. Garanin, Topological Order Generated by a Random Field in a 2d Exchange Model, *Phys. Rev. Lett.* **121**, 017201 (2018).
- [27] E. M. Chudnovsky and D. A. Garanin, Skyrmion glass in a 2D Heisenberg ferromagnet with quenched disorder, *New J. Phys.* **20**, 033006 (2018).
- [28] A. Abanov and V. L. Pokrovsky, Skyrmion in a real magnetic film, *Phys. Rev. B* **58**, R8889 (1998).
- [29] U. K. Röbber, N. Bogdanov, and C. Pfleiderer, Spontaneous skyrmion ground states in magnetic metals, *Nature* **442**, 797 (2006).
- [30] S. Heinze, K. von Bergmann, M. Menzel, J. Brede, A. Kubetzka, R. Wiesendanger, G. Bihlmayer, and S. Blugel, Spontaneous atomic-scale magnetic skyrmion lattice in two dimensions, *Nat. Phys.* **7**, 713 (2011).
- [31] A. O. Leonov and M. Mostovoy, Multiply periodic states and isolated skyrmions in an anisotropic frustrated magnet, *Nat. Commun.* **6**, 8275 (2015).
- [32] G. Chen, A. Mascaraque, A. T. N'Diaye, and A. K. Schmid, Room temperature skyrmion ground state stabilized through interlayer exchange coupling, *Appl. Phys. Lett.* **106**, 242404 (2015).
- [33] O. Boulle, J. Vogel, H. Yang, S. Pizzini, D. de Souza Chaves, A. Locatelli, T. O. Mentès, A. Sala, L. D. Buda-Prejbeanu, O. Klein, M. Belmeguenai, Y. Roussigné, A. Stahkevich, S. M. Chérif, L. Aballe, M. Foerster, M. Chshiev, S. Auffret, I. M. Miron, and G. Gaudin, Room-temperature chiral magnetic skyrmions in ultrathin magnetic nanostructures, *Nat. Nanotech.* **11**, 449 (2016).
- [34] S.-Z. Lin and S. Hayami, Ginzburg-Landau theory for skyrmions in inversion-symmetric magnets with competing interactions, *Phys. Rev. B* **93**, 064430 (2016).
- [35] X. Z. Yu, Y. Tokunaga, Y. Kaneko, W. Z. Zhang, K. Kimoto, Y. Matsui, Y. Taguchi, and Y. Tokura, Biskyrmion states and their current-driven motion in a layered manganite, *Nat. Commun.* **5**, 3198 (2014).
- [36] W. Wang, Y. Zhang, G. Xu, L. Peng, B. Ding, Y. Wang, Z. Hou, X. Zhang, X. Li, E. Liu, S. Wang, J. Cai, F. Wang, J. Li, F. Hu, G. Wu, B. Shen, and X.-X. Zhang, A centrosymmetric hexagonal magnet with superstable biskyrmion magnetic nanodomains in a wide temperature range of 100 – 340K, *Adv. Mater.* **28**, 6887 (2016).
- [37] D. A. Garanin, E. M. Chudnovsky, and X. X. Zhang, Skyrmion clusters from Bloch lines in ferromagnetic films, *Europhys. Lett.* **120**, 17005 (2017).
- [38] X. Zhang, J. Xia, Y. Zhou, X. Liu, and M. Ezawa, Skyrmions and antiskyrmions in a frustrated  $J_1 - J_2 - J_3$  ferromagnetic film: Current-induced helicity locking-unlocking transition, *Nat. Commun.* **8**, 1717 (2017).
- [39] L. Rózsa, K. Palotás, A. Deák, E. Simon, R. Yanes, L. Udvardi, L. Szunyogh, and U. Nowak, Formation and stability of metastable skyrmionic spin structures with various topologies in an ultrathin film, *Phys. Rev. B* **95**, 094423 (2017).
- [40] E. Braaten and L. Carson, Deuteron as a toroidal skyrmion, *Phys. Rev. D* **38**, 3525 (1988).
- [41] W. Y. Crutchfield, N. J. Snyderman, and V. R. Brown, Deuteron in the Skyrme Model, *Phys. Rev. Lett.* **68**, 1660 (1992).
- [42] D. A. Garanin, D. Capic, S. Zhang, X. X. Zhang, and E. M. Chudnovsky, Writing skyrmions with a magnetic dipole, *J. Appl. Phys.* **124**, 113901 (2018).
- [43] A. Derras-Chouk, E. M. Chudnovsky, and D. A. Garanin, Quantum collapse of a magnetic skyrmion, *Phys. Rev. B* **98**, 024423 (2018).
- [44] D. A. Garanin, E. M. Chudnovsky, and T. Proctor, Random field  $xy$  model in three dimensions, *Phys. Rev. B* **88**, 224418 (2013).
- [45] G. Yu, P. Upadhyaya, Q. Shao, H. Wu, G. Yin, X. Li, C. He, W. Jiang, X. Han, P. K. Amiri, and K. Wang, Room-temperature skyrmion shift device for memory application, *Nano Lett.* **17**, 261 (2016).
- [46] W. Legrand, D. Maccariello, N. Reyren, K. Garcia, C. Moutafis, C. Moreau-Luchaire, S. Collin, K. Bouzehouane, V. Cros, and A. Fert, Room-temperature current-induced generation and motion of sub-100 nm skyrmions, *Nano Lett.* **17**, 2703 (2017).
- [47] W. Jiang, P. Upadhyaya, W. Zhang, G. Yu, M. B. Jungfleisch, F. Y. Fradin, J. E. Pearson, Y. Tserkovnyak, K. L. Wang, O. Heinonen, S. G. E. te Velthuis, and A. Hoffmann, Blowing magnetic skyrmion bubbles, *Science* **349**, 283 (2015).
- [48] N. Romming, C. Hanneken, M. Memzel, J. E. Bickel, B. Wolter, K. von Bergmann, A. Kubetzka, and R. Wiesendanger, Writing and deleting single magnetic skyrmions, *Science* **341**, 636 (2013).
- [49] G. Berruto, I. Madan, Y. Murooka, G. M. Vanacore, E. Pomarico, J. Rajeswari, R. Lamb, P. Huang, A. J. Kruchkov, Y. Togawa, T. LaGrange, D. McGrouther, H. M. Ronnow, and F. Carbone, Laser-Induced Skyrmion Writing and Erasing in an Ultrafast Cryo-Lorentz Transmission Electron Microscopy, *Phys. Rev. Lett.* **120**, 117201 (2018).
- [50] S. Zhang, J. Zhang, Q. Zhang, C. Barton, V. Neu, Y. Zhao, Z. Hou, Y. Wen, C. Gong, O. Kazakova, W. Wang, Y. Peng, D. A. Garanin, E. M. Chudnovsky, and X. X. Zhang, Direct writing of room temperature and zero field skyrmion lattices by a scanning local magnetic field, *Appl. Phys. Lett.* **112**, 132405 (2018).
- [51] H. Lavenant, V. Naletov, O. Klein, G. de Loubens, L. Casado, and J. M. de Teresa, Mechanical magnetometry of Cobalt nanospheres deposited by focused electron beam at the tip of ultra-soft cantilever, *Nanofabrication* **1**, 65 (2014); S. Sangiao, C. Magén, D. Mofakhami, G. de Loubens, and J. M. de Teresa, Magnetic properties of optimized cobalt nanospheres grown by focused electron beam induced deposition (FEBID) on cantilever tips, *Beilstein J. Nanotechnol.* **8**, 2106 (2017).
- [52] J. C. Loudon, A. C. Twitchett-Harrison, D. Cortés-Ortuño, M. T. Birch, L. A. Turnbull, A. Štefančič, F. Y. Ogrin, E. O. Burgos-Parra, N. Bukin, A. Laurenson, H. Popescu, M. Beg, O. Hovorka, H. Fangohr, P. A. Medgley, G. Balakrishnan, and P. D. Hatton, Do images of biskyrmions show type-II bubbles? *Adv. Mater.* **31**, 1806598 (2019).
- [53] Y. Yao, B. Ding, J. Cui, X. Shen, Y. Wang, W. Wang, and R. Yu, Magnetic hard nanobubble: A possible magnetic structure behind the bi-skyrmion, *Appl. Phys. Lett.* **114**, 102404 (2019).
- [54] B. Göbel, J. Henk, and I. Mertig, Forming individual magnetic biskyrmions by merging two skyrmions in a centrosymmetric nanodisk, *Nature Sci. Rep.* **9**, 9521 (2019).